Competition between superconductivity and nematic order in high-T_c superconductor

Jing Wang[1] and Guo-Zhu Liu[2,1]

[1]Department of Modern Physics, University of Science and Technology of China, Hefei, Anhui 230026, P. R. China
[2]Max Planck Institut für Physik komplexer Systeme, D-01187 Dresden, Germany

We investigate the competition between superconductivity and nematic order in d-wave high-T_c superconductor. Apart from the competitive interaction with superconducting order, the nematic order also couples strongly to gapless nodal quasiparticles. The interplay of these two interactions is analyzed by means of renormalization group method. An interesting consequence of ordering competition is the appearance of runaway behavior for some specific parameters, which implies an instability of first order transition. We show that the ratio between gap velocity and Fermi velocity, $\kappa = v_\Delta/v_F$, of nodal quasiparticles plays a crucial role in determining the fixed point of the system. As κ decreases, the possibility of first order transition is enhanced. At the nematic critical point where $\kappa \to 0$ driven by the critical nematic fluctuation, no stable fixed point exists and first order transition becomes inevitable. Our results indicate that gapless fermionic degrees of freedom should be taken into account in the theoretical description of competing orders.

PACS numbers: 71.10.Hf, 73.43.Nq, 74.20.De

I. INTRODUCTION

Unconventional superconductors usually refer to the superconductors those can not be understood within the conventional Bardeen-Cooper-Schrieffer (BCS) theory. Notable examples of unconventional superconductors include high-T_c cuprate superconductor, heavy fermion superconductor, and iron-based superconductor. Unlike BCS superconductors, unconventional superconductivity is generally driven by electron-electron interactions, and often has a magnetic origin. Another interesting property of unconventional superconductor is that its ground state is not unique. In addition to the defining superconducting state, unconventional superconductors also exhibit a variety of other symmetry-broken ground states, including antiferromagnetc, nematic, and stripe states, upon tuning such parameters as doping and pressure [1–5]. A widely recognized notion is that the long-range superconducting order competes, and under certain circumstances coexists, with other long-range orders. The competition and possible coexistence between different orders can give rise to rich properties, and hence have attracted intense theoretical and experimental interest in the past years.

The successful microscopic theory of competing orders has not yet been established to date, primarily because the pairing mechanism in most unconventional superconductors is still undetermined. A realistic and commonly used strategy is to build low-energy effective field theory on phenomenological grounds. One can first write down the Ginzburg-Landau (GL) actions for two bosonic order parameters and then introduce certain coupling terms between these two scalar fields. Such generalized GL model has recently been applied to describe competing orders in a number of unconventional superconductors [6–15]. An early success of such theoretical investigation is the prediction of field-induced antiferromagnetic core in the superconducting vortices of high-T_c superconductors [6]. This prediction was subsequently confirmed in experiments [16, 17]. Interestingly, experiments further found that the antiferromagnetic order not only exists in the vortex cores, but also extends into the superconducting region [16] and exhibits nontrivial spatial modulation [17, 18]. A phenomenological field theory that contains a simple quadratic-quadratic coupling term between superconducting and antiferromagnetic order parameters was put forward to understand these new findings [7, 8].

Recently, the issue of competing orders has attracted revived interest. It is found that the competitive interaction between distinct orders can drive an instability, which gives rise to a general tendency of first order transition [11, 14]. This phenomenon may account for the first order transition observed in some unconventional superconductors [4]. In addition, nonuniform glassy electronic phases and Brazovskii type transitions are predicted to emerge due to competition between two long-range orders [10]. Another interesting observation is that the competition between superconducting and antiferromagnetic orders can help to judge the gap symmetry of iron-based superconductors [9, 12]. Furthermore, the competition between superconducting and nematic orders might be responsible for [15] the electronic anisotropy observed in the vortex state of FeSe superconductor [19].

The effective field theory adopted in previous analysis of competing orders normally contains only two bosonic order parameters. The fermionic degrees of freedom are usually completely integrated out in the spirit of Hertz-Millis-Moriya (HMM) theory [20–22]. This integration procedure is expected to be applicable in systems that do not contain gapless fermionic excitations. For instance, the iron-based superconductors seem to have a s-wave energy gap, so the electronic excitations are fully gapped and can be safely integrated out [9, 12]. However, such integration manipulation is not always valid. Indeed, its validity has recently been questioned in several itinerant electron systems [23–26]. In the systems that exhibit gapless fermionic excitations, integrating out fermions may lead to singularities, especially in the vicinity of quantum critical point (QCP). Actually, infrared singularities

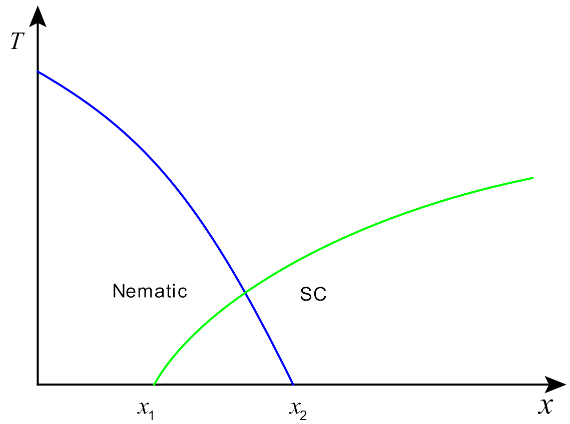

FIG. 1: Schematic phase diagram on (x,T)-plane of high-T_c superconductors. x represents doping concentration. x_1 and x_2 are QCPs of superconducting and nematic phase transitions, repectively.

have been found on the border of several quantum phase transitions [23–26]. In order to properly describe the quantum critical behavior in these systems, it is more appropriate to maintain both bosonic order parameter and gapless fermions in the effective theory. When a long-range order competing with superconductivity also couples to gapless fermions, it would be interesting to go beyond HMM theory and examine the role of gapless fermions. Recent analysis presented in Refs. [13, 27] did suggest nontrivial roles played by gapless fermions.

In various superconductors, superconductivity compete with several possible orders. To examine the role of fermions, we wish to study a prototypical model which describes competition between two distinct long-range orders, contains gapless fermions, and in the meantime is technically controllable. In this paper, we choose to consider competition between superconductivity and nematic order in the contexts of high-T_c superconductors. In recent years, there has been increasing experimental evidence pointing towards the existence of an electronic nematic phase in some high-T_c superconductors [1–3, 28–31], especially $YBa_2Cu_3O_{6+\delta}$ and $Bi_2Sr_2CaCu_2O_{8+\delta}$. According to these experiments, a nematic order is predicted to compete and coexist with superconductivity, which is schematically plotted in Fig. 1. The nematic phase transition and the coupling of nematic fluctuation with fermionic degrees of freedom have stimulated intense research efforts [1–3, 27, 32–41]. From a field-theoretic viewpoint, the nematic order parameter is a simple real scalar field and does not carry finite wave vector, which substantially simplifies theoretical calculations.

It is known that high-T_c superconductor has a $d_{x^2-y^2}$ energy gap, which vanishes at four nodes, $\left(\pm\frac{\pi}{2},\pm\frac{\pi}{2}\right)$. Therefore, gapless nodal quasiparticles (qps) are present even at the lowest energy in the superconducting phase. These nodal qps are believed to be responsible for many anomalous low-temperature properties of the superconducting dome. When a nematic QCP exists somewhere in the superconducting dome, as shown in Fig. 1, the fluctuation of nematic order parameter will couple to these nodal qps. Such coupling can generate non-Fermi liquid behaviors and other unusual phenomena in the vicinity of nematic QCP [27, 36–41]. It may also have significant effects on the interplay between superconductivity and nematic order, which is the topic of this paper.

In the following, we first write down an effective field theory that describes both the competitive interaction between superconducting and nematic order parameters and the coupling between nematic order and nodal qps. We then perform a detailed renormalization group (RG) analysis [42] within such effective theory. In particular, we drive and solve the RG flow equations of all the physical parameters in order to determine the possible stable fixed points. We show that the competitive interaction between superconducting and nematic order parameters still lead to first order transition after including gapless nodal qps. However, the nodal qps do have important impacts on the fixed-point structure. In particular, the velocity ratio κ between gap velocity v_Δ and Fermi velocity v_F of nodal qps turns out to be a crucial controlling parameter. The region that exhibits runaway behavior is greatly enlarged as κ decreases, implying an enhanced possibility of first order transition. At the nematic QCP where $\kappa \to 0$ driven by the critical nematic fluctuation, the system does not have any stable fixed point, so first order transition occurs inevitably. These results clearly indicate the importance of including gapless fermions in the effective field theory of competing orders.

In Sec. II, we write down the effective action which contains two bosonic order parameters and gapless nodal qps. In Sec. III, we make RG calculations and derive the flow equations for all parameters in the effective action. In Sec. IV, we present numerical solutions of the flow equations and discuss the physical implications. The paper is ended in Sec. V with summary and conclusion.

II. EFFECTIVE FIELD THEORY OF COMPETING ORDERS

We first need to write down an effective field theory to describe the competition between superconducting and nematic orders. This will be done largely on phenomenological grounds. In the phase diagram presented in Fig. 1, the horizonal axe is doping concentration x. The QCP of superconducting transition is x_1, which is roughly $x_1 \approx 0.05$ in many high-T_c superconductors. The anticipated QCP for nematic transition is represented by x_2. So far, the precise value, and even the very existence, of x_2 have not yet been unambiguously determined. Here, we assume that x_2 is larger than x_1, which implies a bulk coexistence of superconducting and nematic orders.

In the present system, there are three types of degrees of freedom: superconducting order parameter ψ, nematic order parameter ϕ, and gapless nodal qps Ψ. The competition between superconducting and nematic orders can

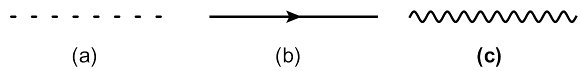

FIG. 2: (a): Free propagator of superconducting field ψ; (b): Free propagator of nematic field ϕ; (c): Free propagator of nodal qps Ψ.

be described by a repulsive quadratic-quadratic coupling term, $\propto \psi^2\phi^2$, which is widely adopted in the description of competing orders. In addition to this competitive interaction, the nematic order parameter ϕ also interacts with gapless nodal qps Ψ, which is usually described by a Yukawa-type coupling term. There is, however, no direct coupling between the superconducting order parameter and nodal qps. First, the nodal qps are excited from the $d_{x^2-y^2}$ gap nodes where superconducting order parameter vanishes. Moreover, these qps are known to have a sharp peak and a very long lifetime in the superconducting dome in the absence of competing orders [43], so their coupling to ψ must be quite weak.

On the basis of the above qualitative analysis, we can write down the following partition function

$$Z = \int \mathcal{D}\psi\mathcal{D}\phi\mathcal{D}\bar{\Psi}\mathcal{D}\Psi e^{S}, \qquad (1)$$

where the effective action is

$$\begin{aligned} S &= S_\psi + S_\phi + S_\Psi + S_{\psi\phi} + S_{\Psi\phi}, &(2)\\ S_\psi &= \frac{1}{2}\int\frac{d^3q}{(2\pi)^3}(-2\alpha+q^2)\psi^2 + \frac{\beta}{2}\int d^2\mathbf{r}d\tau\psi^4, &(3)\\ S_\phi &= \frac{1}{2}\int\frac{d^3q}{(2\pi)^3}\left(-2r+q^2\right)\phi^2 + \frac{u}{2}\int d^2\mathbf{r}d\tau\phi^4, &(4)\\ S_\Psi &= \int\frac{d^3k}{(2\pi)^3}[\Psi_{1i}^\dagger(-i\omega+v_Fk_x\tau^z+v_\Delta k_y\tau^x)\Psi_{1i} \\ &\quad +\Psi_{2i}^\dagger(-i\omega+v_Fk_y\tau^z+v_\Delta k_x\tau^x)\Psi_{2i}], &(5)\\ S_{\psi\phi} &= \gamma\int d^2xd\tau\psi^2\phi^2, &(6)\\ S_{\Psi\phi} &= \int d^2xd\tau[\lambda_0\phi(\Psi_{1i}^\dagger\tau^x\Psi_{1i}+\Psi_{2i}^\dagger\tau^x\Psi_{2i})], &(7)\end{aligned}$$

where $\tau^{x,y,z}$ are Pauli matrices and the flavor index i sums up 1 to N. $\Psi_1^\dagger$ represents nodal QPs excited from $(\frac{\pi}{2},\frac{\pi}{2})$ and $(-\frac{\pi}{2},-\frac{\pi}{2})$ points, and $\Psi_2^\dagger$ the other two. The physical flavor of nodal qps, $N=2$. Here, r is tuning parameter for nematic transition with $r=0$ at x_2. $v_{F,\Delta}$ are the Fermi velocity and gap velocity of nodal qps, respectively. The competitive interaction term $\psi^2\phi^2$ has a positive coefficient, $\gamma>0$. The propagators are shown in Fig. (2). In order to simplify calculations, it proves convenient to make two transformations [37]: $\phi\to\phi/\lambda_0$, and $r\to\lambda_0^2r$. It is now easy to rewrite Eq. (7) as

$$S_{\Psi\phi} = \int d^2xd\tau\phi(\Psi_{1i}^\dagger\tau^x\Psi_{1i}+\Psi_{2i}^\dagger\tau^x\Psi_{2i}). \qquad (8)$$

The effective action represented by Eq. (2) was studied recently in Ref. [27]. It was demonstrated that both superfluid density and critical temperature T_c are significantly suppressed at nematic QCP x_2. However, the superconducting order parameter ψ was assumed in Ref. [27] to be classical, which is valid only when x_2 is not close to x_1. In this paper, we go beyond such approximation and consider the quantum fluctuations of both superconducting and nematic order parameters.

As emphasized in Ref. [27], the gapless nodal qps can have important impacts on the competition between superconductivity and nematic order. The simplest way to include the fermionic degrees of freedom is to introduce the polarization function $\Pi(q)$ due to nodal qps into the effective action of nematic order, S_ϕ. To the leading order of $1/N$-expansion, the polarization function $\Pi(q)$ is represented by the one-loop Feynman diagram shown in Fig. 3(a) and formally given by [37, 41]

$$\Pi(\epsilon,\mathbf{q}) = N\int\frac{d\omega d^2\mathbf{k}}{(2\pi)^3}\mathrm{Tr}[\tau^xG_0(\omega,\mathbf{k})\tau^xG_0(\omega+\epsilon,\mathbf{k}+\mathbf{q})],$$

where

$$G_0(\omega,\mathbf{k}) = \frac{1}{-i\omega+v_Fk_x\tau^z+v_\Delta k_y\tau^x}$$

is the free propagator for nodal QPs Ψ_1 (free propagator for nodal QPs Ψ_2 can be similarly written down). The polarization function $\Pi(\epsilon,\mathbf{q})$ has already been calculated previously [27, 37], and is known to have the form

$$\Pi(\epsilon,\mathbf{q}) = \frac{N}{16v_Fv_\Delta}\left[\frac{\epsilon^2+v_F^2q_x^2}{(\epsilon^2+v_F^2q_x^2+v_\Delta^2q_y^2)^{1/2}}+(q_x\leftrightarrow q_y)\right]. \qquad (9)$$

After including this term, the quadratic part of S_ϕ becomes

$$\left(-2r+q^2\right)\phi^2 \to \left[-2r+q^2+\Pi(q)\right]\phi^2. \qquad (10)$$

From the expression of polarization $\Pi(q)$, it is easy to see that inclusion of $\Pi(q)$ does not change the dynamical exponent $z=1$ of ϕ. However, $\Pi(q)\propto q$, so it dominates over the kinetic term q^2 in the low energy regime. More importantly, the polarization $\Pi(q)$ introduces two important quantities, nodal qps' Fermi velocity v_F and gap velocity v_Δ, into the effective action of ϕ.

Although the polarization $\Pi(q)$ represents the influence of nodal qps, we can not completely integrate the nodal qps out and drop them from the effective theory. These gapless nodal qps should be maintained for several reasons. First, according to the general spirit of RG, one can safely integrate out high-energy modes at low energies. However, the nodal qps are gapless and hence exist even at the lowest energy. Integrating out gapless fermions completely may lead to unphysical singularities. Second, the coupling of gapless fermions with order parameter fluctuation can lead to non-Fermi liquid behavior in observable quantities. In the specific case of nematic transition, the critical nematic fluctuation causes unusual fermion velocity renormalization and extreme anisotropy,

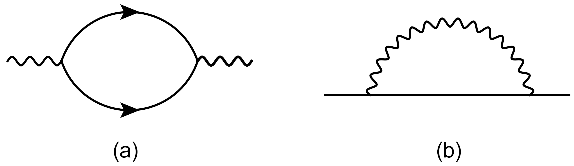

FIG. 3: (a): Polarization function for nematic field ϕ; (b): Fermion self-energy correction due to nematic fluctuation.

which would be overlooked if gapless fermions are fully integrated out. As will be shown below, the velocity ratio $\kappa = v_\Delta/v_F$ play nontrivial roles.

The effective field theory contains seven parameters: $\alpha, r, \beta, u, \gamma, v_F, v_\Delta$. They are all subjected to renormalizations due to the mutual interactions among three field operators: ψ, ϕ, and Ψ. We will study the flow of these seven parameters under scaling transformations and eventually obtain seven RG equations. Since we study the ψ-ϕ interaction and Ψ-ϕ interaction on equal footings, these seven RG equations are self-consistently coupled to each other. The low-energy behaviors of these parameters and the possible fixed points of the effective field theory can be determined by solving these coupled RG equations.

III. RENORMALIZATION GROUP CALCULATIONS

In this section, we make a RG analysis and obtain the flow equations of all the aforementioned parameters. In order to examine the impacts of gapless nodal qps, we go beyond the HMM theory and maintain nodal qps throughout our calculations. We first analyze the coupling between nematic order and nodal qps, and derive the RG equations for fermion velocities, $v_{F,\Delta}$. We then consider the competitive interaction between superconducting and nematic order parameters, and obtain the RG equations for the rest five parameters, $(\alpha, r, \beta, u, \gamma)$, which depend on the fermion velocities, $v_{F,\Delta}$. These seven equations are self-consistently coupled to each other since $v_{F,\Delta}$ appearing in equations of $(\alpha, r, \beta, u, \gamma)$ flow according to their own equations.

A. Flow equations of v_F and v_Δ

The Yukawa-type interaction between nematic order and gapless nodal qps has been recently investigated in several papers [27, 36–41]. It is well-known that the Fermi velocity of nodal qps is not equal to the gap velocity, i.e., $v_F \neq v_\Delta$. Experiments [43, 44] have determined that the velocity ratio $\kappa = v_\Delta/v_F \approx 0.1$. This ratio is a very important parameter since it enters into a number of observable quantities of high-T_c superconductors, including electric conductivity [45, 46], thermal conductivity [46], superfluid density [46, 47], and T_c [47]. An interesting property revealed and discussed in Refs. [27, 36–41] is that the velocity anisotropy is significantly enhanced by the nematic fluctuation.

The calculation of nodal qps self-energy function and the derivation of flow equations have already been presented in previous publications [37, 41], and therefore are not shown here. It is only necessary to summarize the basic calculations as well as the relevant results. To the leading order, the fermion self-energy is represented by the diagram Fig. 3(b), and has the form

$$\Sigma(\omega, \mathbf{k}) = \int \frac{d\epsilon d^2\mathbf{q}}{(2\pi)^3} G_0(\omega+\epsilon, \mathbf{k}+\mathbf{q}) \frac{1}{q^2 + \Pi(q)}. \quad (11)$$

As shown in Ref. [37], it can be written as

$$\frac{d\Sigma(\mathbf{k},\omega)}{d\ln\Lambda} = C_1(-i\omega) + C_2 v_F k_x \tau^z + C_3 v_\Delta k_y \tau^x, \quad (12)$$

where

$$\begin{aligned} C_1 &= \frac{2(v_\Delta/v_F)}{N\pi^3}\int_{-\infty}^{\infty} dx \int_0^{2\pi} d\theta \mathcal{G}(x,\theta) \\ &\times \frac{x^2 - \cos^2\theta - (v_\Delta/v_F)^2 \sin^2\theta}{(x^2+\cos^2\theta + (v_\Delta/v_F)^2\sin^2\theta)^2}, \quad (13) \\ C_2 &= \frac{2(v_\Delta/v_F)}{N\pi^3}\int_{-\infty}^{\infty} dx \int_0^{2\pi} d\theta \mathcal{G}(x,\theta) \\ &\times \frac{\cos^2\theta - x^2 - (v_\Delta/v_F)^2 \sin^2\theta}{(x^2+\cos^2\theta + (v_\Delta/v_F)^2\sin^2\theta)^2}, \quad (14) \\ C_3 &= \frac{2(v_\Delta/v_F)}{N\pi^3}\int_{-\infty}^{\infty} dx \int_0^{2\pi} d\theta \mathcal{G}(x,\theta) \\ &\times \frac{x^2 + \cos^2\theta - (v_\Delta/v_F)^2 \sin^2\theta}{(x^2+\cos^2\theta + (v_\Delta/v_F)^2\sin^2\theta)^2}, \quad (15) \\ \mathcal{G}^{-1} &= \frac{x^2+\cos^2\theta}{\sqrt{x^2+\cos^2\theta+(v_\Delta/v_F)^2\sin^2\theta}} \\ &+ \frac{x^2+\sin^2\theta}{\sqrt{x^2+\sin^2\theta+(v_\Delta/v_F)^2\cos^2\theta}}, \quad (16) \end{aligned}$$

Using Dyson equation, it is easy to get a renormalized fermion propagator

$$G_\psi^{-1}(\mathbf{k},\omega) = -i\omega + v_F k_x \tau^z + v_\Delta k_y \tau^x - \Sigma(\mathbf{k},\omega), \quad (17)$$

which leads to the following RG equations,

$$\begin{aligned} \frac{dv_F}{dl} &= (C_1 - C_2) v_F, \quad (18) \\ \frac{dv_\Delta}{dl} &= (C_1 - C_3) v_\Delta, \quad (19) \\ \frac{d(v_\Delta/v_F)}{dl} &= (C_2 - C_3)(v_\Delta/v_F), \quad (20) \end{aligned}$$

where $l > 0$ is running scale. A straightforward analysis showed that the ratio v_Δ/v_F flows to zero at the lowest energy, giving rise to a novel fixed point of extreme

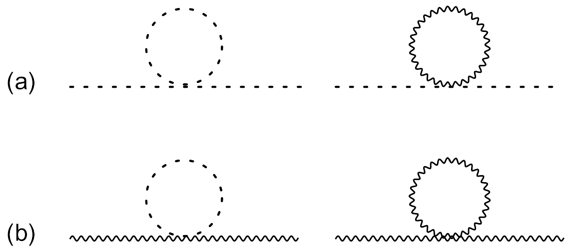

FIG. 4: One-loop corrections to mass parameters α in (a) and r in (b), respectively.

velocity anisotropy [37]. Such fixed point in turn leads to a number of nontrivial consequences, such as unusual broadening of spectral function [36], non-Fermi liquid behavior [38], enhancement of dc thermal conductivity [39], and suppression of superconductivity [27]. To analyze the influence of velocity renormalization and especially the extreme anisotropy manifested at nematic QCP on the nature of superconducting transition, we require that the constant fermion velocities appearing in the polarization $\Pi(q)$ to flow with running scale l according to Eqs. (18) and (19).

The extreme velocity anisotropy is a special feature of the nematic QCP, where $r = 0$ and the nematic fluctuation is critical. Away from nematic QCP, $r \neq 0$, so the nematic fluctuation leads only to relatively unimportant renormalization of fermion velocities. For $r \neq 0$, $v_{F,\Delta}$ and therefore their ratio v_Δ/v_F remain finite.

B. Flow equations of α, r, β, u, and γ

We next consider the competitive interaction between nematic and superconducting order parameters. Our analysis follows closely the scheme presented in a recent work of She *et al.* [14]. It was assumed in Ref. [14] that all the fermionic degrees of freedom can be integrated out and their effects can be represented by the dynamical exponent z. Compared with Ref. [14], the main difference here is the inclusion of polarization $\Pi(q)$ in the effective action of nematic order ϕ, which is supposed to reflect the influence of nodal qps. The corresponding (sub)action that describes ordering competition is

$$S_{\mathrm{com}} = S_\psi + S_\phi + S_{\psi\phi}, \tag{21}$$

where

$$\begin{aligned} S_\psi &= \frac{1}{2}\int \frac{d^2\mathbf{k}d\omega}{(2\pi)^3}\left(-2\alpha + \mathbf{k}^2 + \omega^2\right)\psi^2 \\ &\quad + \frac{\beta}{2}\int \prod_{m=1}^{4} \frac{d^2\mathbf{k}_m d\omega_m}{(2\pi)^3}\delta^2\left(\sum \mathbf{k}_m\right)\delta\left(\sum \omega_m\right)\psi^4, \\ S_\phi &= \int \frac{d^2\mathbf{q}d\epsilon}{(2\pi)^3}\frac{1}{2}\left[-2r + \mathbf{q}^2 + \epsilon^2 + \Pi(q)\right]\phi^2 \\ &\quad + \frac{u}{2}\int \prod_{m=1}^{4} \frac{d^2\mathbf{q}_m d\epsilon_m}{(2\pi)^3}\delta^2\left(\sum \mathbf{q}_m\right)\delta\left(\sum \epsilon_m\right)\phi^4, \\ S_{\psi\phi} &= \gamma\int \prod_{i=1,2} \frac{d^2\mathbf{k}_i d\omega_i d^2\mathbf{q}_i d\epsilon_i}{(2\pi)^6}\psi(\mathbf{k}_i,\omega_i)\phi(\mathbf{q}_i,\epsilon_i) \\ &\quad \times\delta^2\left(\mathbf{k}_1 + \mathbf{k}_2 + \mathbf{q}_1 + \mathbf{q}_2\right)\delta\left(\omega_1 + \omega_2 + \epsilon_1 + \epsilon_2\right). \end{aligned}$$

Before performing a standard RG analysis within this action, it is convenient to rescale momenta and energy by Λ, i.e, $\mathbf{k} \to \mathbf{k}/\Lambda$, $\omega \to \omega/\Lambda$.

According to the sprit of RG theory [14, 27, 37, 41, 42], we employ the following scaling transformations:

$$k_i = k_i' e^{-l}, \tag{22}$$
$$\omega = \omega' e^{-l}, \tag{23}$$
$$\psi(\mathbf{k},\omega) = \psi'(\mathbf{k}',\omega')e^{5l/2}; \tag{24}$$
$$q_i = q_i' e^{-l}, \tag{25}$$
$$\epsilon = \epsilon' e^{-l}, \tag{26}$$
$$\phi(\mathbf{q},\epsilon) = \phi'(\mathbf{q}',\epsilon')e^{5l/2}; \tag{27}$$

where $i = x, y$. Applying these RG transformations, we will be able to derive the RG flow equations for the parameters α, β, r, u, and γ.

Each field operator can be separated into slow mode and fast mode, i.e.,

$$\psi = \psi_s + \psi_f, \tag{28}$$
$$\phi = \phi_s + \phi_f. \tag{29}$$

After introducing an UV cutoff Λ, we can define the slow mode of superconducting order parameter as $\psi_s = \psi(k)$ with $0 < k < e^{-l}\Lambda$ and the fast mode as $\psi_f = \psi(k)$ with $e^{-l}\Lambda < k < \Lambda$, using the formalism of Ref. [42]. Based on such modes separation, the effective action (21) is decomposed into three parts: S^s that contains only slow modes, S^f that contains only fast modes, and S^{sf} that contains both slow and fast modes. More concretely, we have

$$\begin{aligned} S_{\mathrm{com}} &= S^s + S^f + S^{sf} \\ &= \left(S_\psi^s + S_\phi^s + S_{\psi\phi}^s\right) + \left(S_\psi^f + S_\phi^f\right) + S^{sf}, \end{aligned} \tag{30}$$

where

$$\begin{aligned} S_\psi^s &= \frac{1}{2}\int \frac{d^2\mathbf{k}d\omega}{(2\pi)^3}\left(-2\alpha + \mathbf{k}^2 + \omega^2\right)\psi_s^2 \\ &\quad + \frac{\beta}{2}\int \prod_{m=1}^{4} \frac{d^2\mathbf{k}_m d\omega_m}{(2\pi)^3}\delta^2\left(\sum \mathbf{k}_m\right)\delta\left(\sum \omega_m\right)\psi_s^4, \\ S_\phi^s &= \frac{1}{2}\int \frac{d^2\mathbf{q}d\epsilon}{(2\pi)^3}\left[-2r + \mathbf{q}^2 + \epsilon^2 + \Pi(q)\right]\phi_s^2 \\ &\quad + \frac{u}{2}\int \prod_{m=1}^{4} \frac{d^2\mathbf{q}_m d\epsilon_m}{(2\pi)^3}\delta^2\left(\sum \mathbf{q}_m\right)\delta\left(\sum \epsilon_m\right)\phi_s^4, \\ S_{\psi\phi}^s &= \gamma\int \prod_{i=1,2} \frac{d^2\mathbf{k}_i d\omega_i d^2\mathbf{q}_i d\epsilon_i}{(2\pi)^6}\psi(\mathbf{k}_i,\omega_i)\phi(\mathbf{q}_i,\epsilon_i) \\ &\quad \times\delta^2\left(\mathbf{k}_1 + \mathbf{k}_2 + \mathbf{q}_1 + \mathbf{q}_2\right)\delta\left(\omega_1 + \omega_2 + \epsilon_1 + \epsilon_2\right); \end{aligned}$$

$$S_\psi^f = \frac{1}{2}\int \frac{d^2\mathbf{k}d\omega}{(2\pi)^3}\left(-2\alpha + \mathbf{k}^2 + \omega^2\right)\psi_f^2 + \frac{\beta}{2}\int\prod_{m=1}^{4}\frac{d^2\mathbf{k}_m d\omega_m}{(2\pi)^3}\delta^2\left(\sum \mathbf{k}_m\right)\delta\left(\sum\omega_m\right)\psi_f^4,$$

$$S_\phi^f = \frac{1}{2}\int \frac{d^2\mathbf{q}d\epsilon}{(2\pi)^3}\left[-2r + \mathbf{q}^2 + \epsilon^2 + \Pi(q)\right]\phi_f^2 + \frac{u}{2}\int\prod_{m=1}^{4}\frac{d^2\mathbf{q}_m d\epsilon_m}{(2\pi)^3}\delta^2\left(\sum \mathbf{q}_m\right)\delta\left(\sum\epsilon_m\right)\phi_f^4,$$

$$\begin{aligned} S^{sf} &= \int \frac{d^2\mathbf{k}d\omega}{(2\pi)^3}\frac{3}{2}\left(\beta\psi_f\psi_f\psi_s\psi_s + u\phi_f\phi_f\phi_s\phi_s\right) \\ &+ \int\prod_{i=1,2}\frac{d^2\mathbf{k}_i d\omega_i d^2\mathbf{q}_i d\epsilon_i}{(2\pi)^6}\delta^2\left(\mathbf{k}_1+\mathbf{k}_2+\mathbf{q}_1+\mathbf{q}_2\right) \\ &\times\delta\left(\omega_1+\omega_2+\epsilon_1+\epsilon_2\right)\left(\gamma\psi_s\psi_s\phi_f\phi_f\right. \\ &\left.+\gamma\psi_f\psi_f\phi_s\phi_s + 4\gamma\psi_f\psi_s\phi_f\phi_s\right).\end{aligned}$$

After this decomposition, now the partition function can be rearranged in the following way,

$$\begin{aligned} Z &= \int \mathcal{D}\psi_s\mathcal{D}\phi_s\mathcal{D}\bar{\Psi}\mathcal{D}\Psi\int\mathcal{D}\psi_f\mathcal{D}\phi_f \\ &\times\exp\left[\left(S_\psi^s + S_\phi^s + S_{\psi\phi}^s\right) + \left(S_\psi^f + S_\phi^f\right) + S^{sf}\right] \\ &= \int \mathcal{D}\psi_s\mathcal{D}\phi_s\mathcal{D}\bar{\Psi}\mathcal{D}\Psi\exp\left(S_\psi^s + S_\phi^s + S_{\psi\phi}^s\right) \\ &\times\int\mathcal{D}\psi_f\mathcal{D}\phi_f\exp\left[\left(S_\psi^f + S_\phi^f\right) + S^{sf}\right] \\ &= \int \mathcal{D}\psi_s\mathcal{D}\phi_s\mathcal{D}\bar{\Psi}\mathcal{D}\Psi\exp\left(S_\psi'^s + S_\phi'^s + S_{\psi\phi}'^s\right) \\ &\equiv \int \mathcal{D}\psi_s\mathcal{D}\phi_s\mathcal{D}\bar{\Psi}\mathcal{D}\Psi\exp\left(S'_{\mathrm{eff}}\right). \end{aligned} \tag{31}$$

The next step is to integrate over all the fast modes, and obtain an effective action of slow modes. The functional integration can be performed using the standard diagrammatic techniques. The propagators for the superconducting order ψ and the nematic order ϕ, shown in Fig. (2), are

$$G_\psi(\mathbf{k},\omega) = \frac{1}{-2\alpha + \mathbf{k}^2 + \omega^2}, \tag{32}$$

$$G_\phi(\mathbf{q},\epsilon) = \frac{1}{-2r + \mathbf{q}^2 + \epsilon^2 + \Pi(q)}. \tag{33}$$

The polarization appearing in $G_\phi(\mathbf{q},\epsilon)$ reflects the presence of gapless nodal qps. As already pointed out, $\Pi(q)$ dominates over the kinetic term q^2 in the low-energy regime. In order to further simplify the nematic propagator, we consider the close vicinity of nematic QCP where r is very small. In this case, we are allowed to approximate the nematic propagator by

$$\begin{aligned} G_\phi(\mathbf{q},\epsilon) &\approx \frac{1}{-2r + \Pi(q)} \\ &\approx \frac{1}{\Pi(q)\left(1 - \frac{2r}{\Pi(q)}\right)} \\ &\approx \frac{1}{\Pi(q)} + \frac{2r}{\Pi^2(q)}. \end{aligned} \tag{34}$$

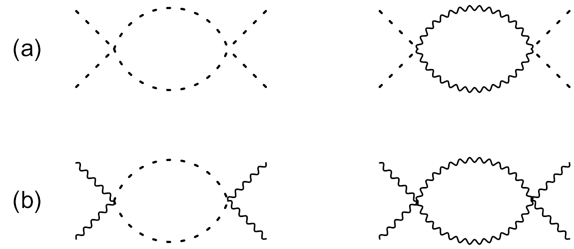

FIG. 5: One-loop corrections to quartic coefficients β in (a) and u in (b), respectively.

This expansion is apparently inappropriate when r is not small. For large r, it is better to consider $\Pi(q)/r$ as small expanding parameter, which will be discussed later.

Now let us work in the spherical coordinates. We first define $\epsilon \equiv vq_0 = vq\cos\theta$, $q_1 = q\sin\theta\cos\varphi$, and $q_2 = q\sin\theta\sin\varphi$, with v being the velocity of nematic order parameter ϕ. For convenience, we could extract constant v from the energy ω of superconducting order parameter ψ. Accordingly, the velocities of nodal qps, v_F and v_Δ, can be divided by v. After this manipulation, v_F and v_Δ become dimensionless. Now the polarization function can be written in the form,

$$\Pi(q,\theta,\varphi) = qD(\theta,\varphi), \tag{35}$$

where the function

$$\begin{aligned} D(\theta,\varphi) &= \frac{1}{16v_F v_\Delta} \\ &\times\left(\frac{\cos^2\theta + v_F^2\sin^2\theta\cos^2\varphi}{\sqrt{\cos^2\theta + v_F^2\sin^2\theta\cos^2\varphi + v_\Delta^2\sin^2\theta\sin^2\varphi}}\right. \\ &+\left.\frac{\cos^2\theta + v_F^2\sin^2\theta\sin^2\varphi}{\sqrt{\cos^2\theta + v_F^2\sin^2\theta\sin^2\varphi + v_\Delta^2\sin^2\theta\cos^2\varphi}}\right) \end{aligned}$$

is dimensionless. Before proceeding with the next calculations, it is helpful to define

$$F_1 \equiv F_1(v_F, v_\Delta) = \int_0^\pi d\theta\int_0^{2\pi}d\varphi\frac{\sin\theta}{(2\pi)^3 D(\theta,\varphi)}, \tag{36}$$

$$F_2 \equiv F_2(v_F, v_\Delta) = \int_0^\pi d\theta\int_0^{2\pi}d\varphi\frac{\sin\theta}{(2\pi)^3 D^2(\theta,\varphi)}, \tag{37}$$

$$F_3 \equiv F_3(v_F, v_\Delta) = \int_0^\pi d\theta\int_0^{2\pi}d\varphi\frac{\sin\theta}{(2\pi)^3 D^3(\theta,\varphi)}. \tag{38}$$

With these arrangements, we can now turn to calculate the one-loop contribution to the RG equations of all parameters.

C. α, r

The diagrams contributing to α to leading order are shown in Fig. 4(a). We perform the following calculations,

$$\begin{aligned} S[\alpha] &= \int^b \frac{d^3q}{(2\pi)^3}\psi_s(q)\psi_s(-q)\left[-2\alpha+3\beta\int_b^1\frac{d^3q'}{(2\pi)^3}G_\psi^f\right. \\ &\quad \left. +\gamma\int_b^1\frac{d^3q'}{(2\pi)^3}G_\phi^f\right] \\ &\approx \int^b\frac{d^3q}{(2\pi)^3}\psi_s(q)\psi_s(-q)(-2\alpha) \\ &\quad \times\exp\left\{-\frac{l}{2\alpha}\left[\frac{3\beta}{2\pi^2}(1+2\alpha)+\gamma\left(F_1+2rF_2\right)\right]\right\} \\ &= \int^1\frac{d^3q}{(2\pi)^3}e^{-3l}\psi_s(q)\psi_s(-q)e^{5l/2}e^{5l/2}(-2\alpha) \\ &\quad \times\exp\left\{-\frac{l}{2\alpha}\left[\frac{3\beta}{2\pi^2}(1+2\alpha)+\gamma(F_1+2rF_2)\right]\right\} \\ &\equiv \int^1\frac{d^3q}{(2\pi)^3}\psi_s(q)\psi_s(-q)(-2\alpha'), \end{aligned} \tag{39}$$

where

$$\alpha' = \alpha\exp\left\{2l-\frac{l}{2\alpha}\left[\frac{3\beta}{2\pi^2}(1+2\alpha)+\gamma(F_1+2rF_2)\right]\right\}.$$

Its derivative with respect to running scale l is

$$\frac{d\alpha}{dl} = 2\alpha-\left[\frac{3\beta}{4\pi^2}(1+2\alpha)+\frac{\gamma}{2}(F_1+2rF_2)\right]. \tag{40}$$

By calculating the diagrams shown in Fig. 4(b), the flow equation for parameter r can be obtained similarly,

$$\frac{dr}{dl} = 2r-\left[\frac{3u}{2}(F_1+2rF_2)+\frac{\gamma}{4\pi^2}(1+2\alpha)\right]. \tag{41}$$

In the absence of fermionic degrees of freedom, $F_1 = F_2 = \frac{1}{2\pi^2}$, then the flow equation of α is identical to that of r [14]. Such an "exchange symmetry" is certainly broken by gapless nodal qps via the polarization $\Pi(q)$ appearing in the effective action of nematic order ϕ.

D. β, u

The one-loop corrections to β are depicted in Fig. 5(a). By paralleling the steps performed in Eq. (39), we can similarly obtain

$$S[\beta] \equiv \int^1\prod_{m=1}^4\frac{d^2\mathbf{k}_m d\omega_m}{(2\pi)^3}\delta^2\left(\sum\mathbf{k}_m\right)\delta\left(\sum\omega_m\right)\frac{\beta'}{2}|\psi_s|^4,$$

where

$$\beta' = \beta\exp\left\{1-\frac{2}{\beta}\left[\frac{9\beta^2}{2\pi^2}+\gamma^2(F_2+4rF_3)\right]\right\}l.$$

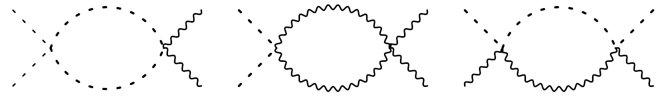

FIG. 6: One-loop corrections to coupling constant γ.

It leads to

$$\frac{d\beta}{dl} = \beta-\left[\frac{9\beta^2}{\pi^2}+2\gamma^2(F_2+4rF_3)\right]. \tag{42}$$

By calculating diagrams shown in Fig. 5(b), the RG equation for u is found to be

$$\frac{du}{dl} = u-\left[\frac{\gamma^2}{\pi^2}+18u^2(F_2+4rF_3)\right]. \tag{43}$$

Once again, the influence of gapless nodal qps is reflected in the functions $F_{2,3}$.

E. γ

Now we consider the flow of γ, which characterizes the strength of competitive interaction. The one-loop corrections to the term $\gamma\psi^2\phi^2$ has three diagrams, presented in Fig. (6). Following similar procedure, we eventually obtain

$$S[\gamma] \equiv \int^1\prod_{m=1}^4\frac{d^2\mathbf{k}_m}{(2\pi)^2}\frac{d\omega_m}{2\pi}\delta^2\left(\sum\mathbf{k}_m\right)\delta\left(\sum\omega_m\right)\gamma'\psi_s^2\phi_s^2,$$

where

$$\begin{aligned} \gamma' &= \gamma\exp\Big\{l-\Big[\frac{3\beta}{\pi^2}+6u(F_2+4rF_3). \\ &\quad +8\gamma\left(F_1+F_2 2r+F_1 2\alpha\right)\Big]l\Big\}. \end{aligned}$$

The flow equation of γ is therefore given by

$$\begin{aligned} \frac{d\gamma}{dl} &= \gamma\Big\{1-\Big[\frac{3\beta}{\pi^2}+6u(F_2+4rF_3) \\ &\quad +8\gamma\left(F_1+F_2 2r+F_1 2\alpha\right)\Big]\Big\}. \end{aligned} \tag{44}$$

IV. NUMERICAL RESULTS AND PHYSICAL IMPLICATIONS

In order to specify the possible fixed point of the system under consideration, we need to solve the RG equations. For later reference, it is useful to list all the RG equations obtained in the previous section,

$$\frac{d\alpha}{dl} = 2\alpha-\left[\frac{3\beta}{4\pi^2}(1+2\alpha)+\frac{\gamma}{2}(F_1+2rF_2)\right], \tag{45}$$

$$\frac{dr}{dl} = 2r-\left[\frac{3u}{2}(F_1+2rF_2)+\frac{\gamma}{4\pi^2}(1+2\alpha)\right], \tag{46}$$

$$\frac{d\beta}{dl} = \beta - \left[\frac{9\beta^2}{\pi^2} + 2\gamma^2(F_2 + 4rF_3)\right], \quad (47)$$

$$\frac{du}{dl} = u - \left[\frac{\gamma^2}{\pi^2} + 18u^2(F_2 + 4rF_3)\right], \quad (48)$$

$$\frac{d\gamma}{dl} = \gamma\Big\{1 - \Big[\frac{3\beta}{\pi^2} + 6u(F_2 + 4rF_3) + 8\gamma\left(F_1 + F_2 2r + F_1 2\alpha\right)\Big]\Big\}, \quad (49)$$

$$\frac{dv_F}{dl} = (C_1 - C_2)v_F, \quad (50)$$

$$\frac{dv_\Delta}{dl} = (C_1 - C_3)v_\Delta. \quad (51)$$

Compared with the case in which the action contains only two bosonic order parameters, the gapless nodal qps show their existence through the three functions $F_{1,2,3}$, which are determined by fermion velocities, $v_{F,\Delta}$. We now address how the velocity ratio affects the fixed point structure of the interacting system.

As already pointed out, extreme velocity anisotropy with $\kappa \to 0$ is a special property of nematic QCP with $r = 0$. For finite r, the velocities receive only unimportant renormalizations, and the ratio κ remains finite. To make our analysis simpler, we first consider the case of finite r and solve the above RG equations by assuming two representative constant values of κ. From the solutions, we will know qualitatively how the fixed point evolves as κ decreases. We then consider nematic QCP with $r = 0$, and solve the flow equations (45, 46, 47, 48, 49) self-consistently after taking into account the extreme anisotropy limit, $\kappa \to 0$.

A. $v_\Delta/v_F = 0.1$

First, we consider a constant $v_\Delta/v_F = 0.1$, which is an appropriate value for the velocity ratio in some realistic high-T_c superconductors [35, 43, 44]. In the presence case, the dimensionless velocity is set to $v_F = 1$ [2], and therefore $v_\Delta = 0.1$. Substituting them into Eq. (36), we have

$$D(\theta,\varphi) = \frac{5}{8}\left(\frac{\cos^2\theta + \sin^2\theta\cos^2\varphi}{\sqrt{\cos^2\theta + \sin\theta^2\cos^2\varphi + 0.01\sin\theta^2\sin^2\varphi}} + \frac{\cos^2\theta + \sin^2\theta\sin^2\varphi}{\sqrt{\cos^2\theta + \sin^2\theta\sin^2\varphi + 0.01\sin^2\theta\cos^2\varphi}}\right),$$

and

$$F_1 = \int_0^\pi d\theta \int_0^{2\pi} d\varphi \frac{\sin\theta}{(2\pi)^3 D(\theta,\varphi)} \approx 0.053, \quad (52)$$

$$F_2 = \int_0^\pi d\theta \int_0^{2\pi} d\varphi \frac{\sin\theta}{(2\pi)^3 D^2(\theta,\varphi)} \approx 0.057, \quad (53)$$

$$F_3 = \int_0^\pi d\theta \int_0^{2\pi} d\varphi \frac{\sin\theta}{(2\pi)^3 D^3(\theta,\varphi)} \approx 0.062. \quad (54)$$

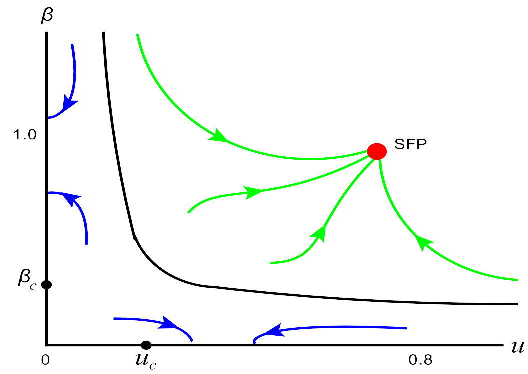

FIG. 7: Schematic diagram of flow trajectories in (β, u) plane for bare velocity ratio $v_\Delta/v_F = 0.1$. The stable fixed point (SFP) is $(\alpha^*, r^*, \beta^*, u^*, \gamma^*) \approx (0.053547, 0.043491, 1.013065, 0.757126, 0.754569)$. When β and/or u fall in the region left to and below the solid critical line, the system under consideration exhibits runaway behavior, indicating the occurrence of first order transition.

Now the RG equations (45, 46, 47, 48, 49) can be approximated as

$$\frac{d\alpha}{dl} = 2\alpha - \left[\frac{3\beta}{4\pi^2}(1+2\alpha) + \frac{\gamma}{2}(0.053 + 0.114r)\right], \quad (55)$$

$$\frac{dr}{dl} = 2r - \left[\frac{3u}{2}(0.053 + 0.114r) + \frac{\gamma}{4\pi^2}(1+2\alpha)\right], \quad (56)$$

$$\frac{d\beta}{dl} = \beta - \left[\frac{9\beta^2}{\pi^2} + 2\gamma^2(0.057 + 0.248r)\right], \quad (57)$$

$$\frac{du}{dl} = u - \left[\frac{\gamma^2}{\pi^2} + 18u^2(0.057 + 0.248r)\right], \quad (58)$$

$$\frac{d\gamma}{dl} = \gamma\Big\{1 - \Big[\frac{3\beta}{\pi^2} + 6u(0.057 + 0.248r) + 8\gamma\left(0.053 + 0.114r + 0.106\alpha\right)\Big]\Big\}. \quad (59)$$

By setting all these derivatives to zero, the fixed points could be determined. After numerical calculations, we find the following solutions (unphysical ones have been discarded):

1) $(\alpha^*, r^*, \beta^*, u^*, \gamma^*) \approx (0.034935, 0.041791, 0.377768, 0.540608, 1.355735)$,

2) $(\alpha^*, r^*, \beta^*, u^*, \gamma^*) \approx (0.040467, 0.035673, 0.487222, 0.374853, 1.433849)$,

3) $(\alpha^*, r^*, \beta^*, u^*, \gamma^*) \approx (0.050708, 0.030099, 0.757159, 0.266773, 1.348298)$,

4) $(\alpha^*, r^*, \beta^*, u^*, \gamma^*) \approx (0.053547, 0.043491, 1.013065, 0.757126, 0.754569)$.

We need to find out the stable fixed point from these four solutions. By fixing $\alpha = \alpha^*, r = r^*, \gamma = \gamma^*$, and making numerical analysis, we find that $(\alpha^*, r^*, \beta^*, u^*, \gamma^*) \approx (0.053547, 0.043491, 1.013065, 0.757126, 0.754569)$ corresponds to the stable fixed point. In fact, we only need to address the physical properties in the vicinity of the stable fixed point. At $\alpha = \alpha^*, r = r^*, \gamma = \gamma^*$, it appears

that the flow trajectories of β and u show runaway behavior when the initial values of β and u are below the critical values $\beta_c \approx 0.0835$ and/or $u_c \approx 0.0625$, which are shown in Fig. (7). As extensively discussed previously [11, 14, 48–50], such runaway behavior implies a first-order phase transition.

B. $v_\Delta/v_F = 0.01$

We then assume that $v_\Delta/v_F = 0.01$, and examine how the fixed point structure is modified as the ratio v_Δ/v_F decreases. In the present case, we have

$$D(\theta,\varphi) = \frac{25}{4}\left(\frac{\cos^2\theta+\sin^2\theta\cos^2\varphi}{\sqrt{\cos^2\theta+\sin^2\theta\cos^2\varphi+0.0001\sin^2\theta\sin^2\varphi}} + \frac{\cos^2\theta+\sin^2\theta\sin^2\varphi}{\sqrt{\cos^2\theta+\sin^2\theta\sin^2\varphi+0.0001\sin^2\theta\cos^2\varphi}}\right)$$

and then

$$F_1 = \int_0^\pi d\theta\int_0^{2\pi} d\varphi\frac{\sin\theta}{(2\pi)^3 D(\theta,\varphi)} \approx 0.005274, \quad (60)$$

$$F_2 = \int_0^\pi d\theta\int_0^{2\pi} d\varphi\frac{\sin\theta}{(2\pi)^3 D^2(\theta,\varphi)} \approx 0.000561, \quad (61)$$

$$F_3 = \int_0^\pi d\theta\int_0^{2\pi} d\varphi\frac{\sin\theta}{(2\pi)^3 D^3(\theta,\varphi)} \approx 0.000062. \quad (62)$$

Hence, the set of RG equations (45, 46, 47, 48, 49) approximately becomes

$$\frac{d\alpha}{dl} = 2\alpha-\left[\frac{3\beta}{4\pi^2}(1+2\alpha)+\frac{\gamma}{2}(0.00527+0.00112r)\right], \quad (63)$$

$$\frac{dr}{dl} = 2r-\left[\frac{3u}{2}(0.00527+0.00112r)+\frac{\gamma}{4\pi^2}(1+2\alpha)\right], \quad (64)$$

$$\frac{d\beta}{dl} = \beta-\left[\frac{9\beta^2}{\pi^2}+2\gamma^2(0.00056+0.00025r)\right], \quad (65)$$

$$\frac{du}{dl} = u-\left[\frac{\gamma^2}{\pi^2}+18u^2(0.00056+0.00025r)\right], \quad (66)$$

$$\frac{d\gamma}{dl} = \gamma\Big\{1-\Big[\frac{3\beta}{\pi^2}+6u(0.00056+0.00025r) +8\gamma(0.00527+0.00112r+0.01055\alpha)\Big]\Big\}. \quad (67)$$

By applying the same methods used in the case of $v_\Delta/v_F = 0.1$, we also find four solutions:
1) $(\alpha^*, r^*, \beta^*, u^*, \gamma^*) \approx (0.053548, 0.437666, 1.013124, 76.671917, 7.590670)$,
2) $(\alpha^*, r^*, \beta^*, u^*, \gamma^*) \approx (0.034916, 0.420692, 0.377357, 54.780339, 13.639865)$,
3) $(\alpha^*, r^*, \beta^*, u^*, \gamma^*) \approx (0.040451, 0.358983, 0.486613, 37.941187, 14.432612)$,
4) $(\alpha^*, r^*, \beta^*, u^*, \gamma^*) \approx (0.050767, 0.302544, 0.758586, 26.941770, 13.562402)$.

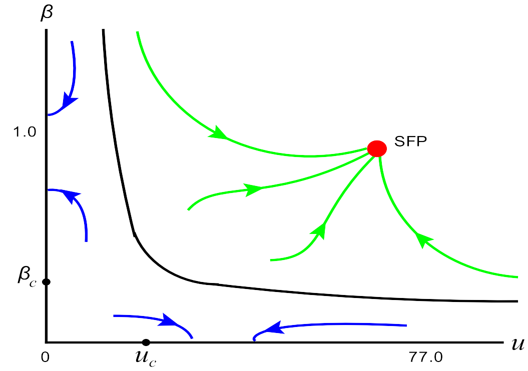

FIG. 8: Schematic diagram of flow trajectories in (β, u) plane for the bare velocity ratio $v_\Delta/v_F = 0.01$. The SFP is $(\alpha^*, r^*, \beta^*, u^*, \gamma^*) \approx (0.053548, 0.437666, 1.013124, 76.671917, 7.590670)$. Compared to the case of $v_\Delta/v_F = 0.1$ (see Fig. 7), the region exhibiting runaway behavior is greatly amplified. It seems that a smaller ratio v_Δ/v_F leads to enhanced possibility of first order transition.

Among these points, only the first is stable. The corresponding critical values of β, u are $\beta_c \approx 0.0833$ and $u_c \approx 6.32$, which are shown in Fig. (8).

Compared with the results obtained at $v_\Delta/v_F = 0.1$, we find that the probability of first-order transition rapidly rises as velocity ratio κ decreases, because the region of runaway behavior is significantly enhanced. It is nature to speculate that first-order transition may be inevitable when the velocity ratio κ vanishes. In order to judge this speculation, we finally consider the nematic QCP where $r = 0$.

C. $r = 0$

At nematic QCP with $r = 0$, the velocity is no longer finite: it becomes scale-dependent, and vanishes at the lowest energy. In this case, we should study the fixed point by self-consistently solving the following equations,

$$\frac{d\alpha}{dl} = 2\alpha-\left[\frac{3\beta}{4\pi^2}(1+2\alpha)+\frac{\gamma}{2}F_1\right]=0, \quad (68)$$

$$\frac{d\beta}{dl} = \beta-\left[\frac{9\beta^2}{\pi^2}+2\gamma^2F_2\right]=0, \quad (69)$$

$$\frac{du}{dl} = u-\left[\frac{\gamma^2}{\pi^2}+18u^2F_2\right]=0, \quad (70)$$

$$\frac{d\gamma}{dl} = \gamma\left\{1-\left[\frac{3\beta}{\pi^2}+6uF_2+8\gamma(F_1+F_1 2\alpha)\right]\right\}=0, \quad (71)$$

$$\frac{dv_F}{dl} = (C_1-C_2)v_F = 0, \quad (72)$$

$$\frac{dv_\Delta}{dl} = (C_1-C_3)v_\Delta = 0, \quad (73)$$

which are obtained at the nematic QCP $r = 0$.

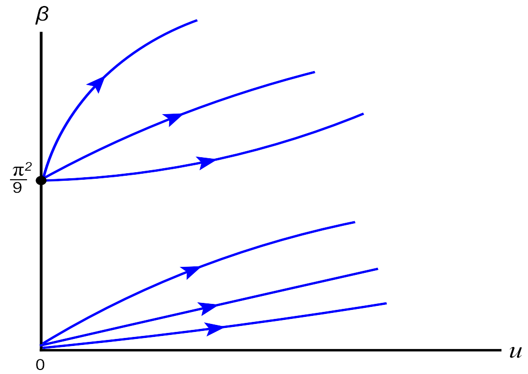

FIG. 9: At nematic QCP with $r = 0$, the velocities $v_{F,\Delta}$ and their ratio v_Δ/v_F all flow to zero due to critical nematic fluctuation at the lowest energy. The system under consideration has no SFP in this case and exhibits runaway behavior in the whole plane of (β, u), so first order transition becomes unavoidable.

Since the equations of v_F, v_Δ are relatively independent of other parameters, they could be first solved. It is easy to get $v_F^* = 0, v_\Delta^* = 0$, which implies that $F_1 = F_2 = F_3 = 0$. The rest equations now become

$$\frac{d\alpha}{dl} = 2\alpha - \frac{3\beta}{4\pi^2}(1+2\alpha) = 0, \tag{74}$$

$$\frac{d\beta}{dl} = \beta - \frac{9\beta^2}{\pi^2} = 0, \tag{75}$$

$$\frac{du}{dl} = u - \frac{\gamma^2}{\pi^2} = 0, \tag{76}$$

$$\frac{d\gamma}{dl} = \gamma\left(1 - \frac{3\beta}{\pi^2}\right) = 0, \tag{77}$$

which have two solutions: 1) $r^* = u^* = \gamma^* = 0$, $\beta^* = \alpha^* = 0$; 2) $r^* = u^* = \gamma^* = 0$, $\beta^* = \frac{\pi^2}{9}, \alpha^* = \frac{1}{22}$.

One can check that both of these two solutions are unstable. Hence, there is no stale fixed point at all at nematic QCP where the velocity ratio v_Δ/v_F vanishes due to critical nematic fluctuation. The corresponding schematic flow diagram is shown in Fig. (9). The runaway behavior is present in the whole region spanned by (β, u), indicating that first-order phase transition always takes place.

Now let us discuss a little more about the role of nodal qps. Within the HMM theory, the fermionic degrees of freedom can be fully integrated out. If we do so in our case, then we would obtain an effective action that consists of solely two bosonic order parameters, ψ and ϕ. The influence of gapless nodal qps is only reflected by the polarization $\Pi(q)$ which contributes a term $\Pi(q)\phi^2$ to the effective Lagrangian. The fermion velocities, $v_{F,\Delta}$, have to take their bare values and can not be renormalized, because the coupling between nematic order and nodal qps is neglected once the nodal qps are completely integrated out. It is therefore not possible to incorporate the extreme velocity anisotropy driven by the critical nematic fluctuation into the theoretical analysis. However, as shown in the above calculations, such extreme velocity anisotropy does have significant effects on the RG trajectories (please compare Fig. 9 with Fig. 7). Apparently, an important indication of results is that gapless nodal qps do play an essential role and therefore should be taken into account in the effective theory of competing orders.

D. Relatively large r

In the above calculations, we have simplified the effective propagator of nematic order parameter, $G_\phi(q)$, in terms of small quantity $r/\Pi(q)$. This expansion is appropriate in the close vicinity of nematic QCP with small r. When r is relatively large, we consider $\Pi(q)/r$ as small parameter and expand $G_\phi(q)$ as

$$\begin{aligned} G_\phi(\mathbf{q},\epsilon) &\approx \frac{1}{-2r + \Pi(q)} \\ &\approx \frac{1}{-2r\left(1 - \frac{\Pi(q)}{2r}\right)} \\ &\approx -\frac{1}{2r} + \frac{\Pi(q)}{4r^2}. \end{aligned} \tag{78}$$

We have performed RG calculations using this propagator for relatively large r, and found that our qualitative conclusion reached above does not change.

V. SUMMARY AND DISCUSSION

In summary, we have performed a RG analysis within an effective field theory of the competition between superconductivity and nematic order in the context of d-wave high-T_c superconductors. Our results confirm the qualitative conclusion of Refs. [14, 21] that ordering competition can generically give rise to first order transition. Different from previous treatments, we go beyond the HMM framework and incorporate gapless nodal qps explicitly in our calculations. It is found that the ratio κ between gap velocity v_Δ and Fermi velocity v_F of nodal qps plays a crucial important role in determining the RG flow diagram of the system. As κ decreases from its bare value, the possibility of first order transition is enhanced. When κ approaches zero at the nematic QCP due to the critical nematic fluctuation, first order transition become inevitable because the system exhibits runaway behavior in the whole space spanned by parameters u and β, the quartic coefficients of superconducting and nematic order parameters respectively. These results indicates that gapless fermionic degrees of freedom can neither be ignored nor fully integrate out.

The competition between superconductivity and nematic order is merely a very simple example of ordering competition. It is more interesting to study the competition between superconductivity and antiferromagnetism, which is a fundamental issue in high-T_c superconductor,

heavy fermion superconductor, and iron-based superconductor. Compared with the case of competing nematic order, the interplay between superconductivity and antiferromagnetism is more complicated and exhibits richer properties. For instance, the antiferromagnetic order parameter is a complex scalar field and carries a finite wave vector **Q** which is often incommensurate. Furthermore, the antiferromagnetic order parameter may acquire a nontrivial dynamical exponent, $z \neq 1$, due to coupling with gapless fermions, which would make RG calculations more involved [14]. Nevertheless, despite these technical difficulties, the general formalism presented in the present paper can be applied to analyze the influence of fermionic degrees of freedom on the interplay between superconductivity and antiferromagnetism.

Acknowledgments

We are grateful to Jian-Huang She for very helpful communications. G.Z.L. acknowledges financial support by the National Natural Science Foundation of China under grant No. 11074234 and the Visitors Program of MPIPKS at Dresden.

[1] S. A. Kivelson, I. P. Bindloss, E. Fradkin, V. Oganesyan, J. M. Tranquada, A. Kapitulnik, and C. Howald, Rev. Mod. Phys. **75**, 1201 (2003).
[2] M. Vojta, Adv. Phys. **58**, 699 (2009).
[3] E. Fradkin, S. A. Kivelson, M. J. Lawler, J. P. Eisenstein, and A. P. Mackenzie, Annu. Rev. Condens. Matter Phys. **1**, 153 (2010); E. Fradkin, arXiv:1004.1104.
[4] P. Gegenwart, Q. Si, and F. Steglich, Nat. Phys. **4**, 186 (2008); O. Stockert, S. Kirchner, F. Steglich, and Q. Si, J. Phys. Soc. Jpn. **81**, 011001 (2012).
[5] G. Knebel, D. Aoki, and J. Flouquet, arXiv:0911.5223.
[6] D. P. Arovas, A. J. Berlinsky, C. Kallin, and S.-C. Zhang, Phys. Rev. Lett. **79**, 2871 (1997).
[7] E. Demler, S. Sachdev, and Y. Zhang, Phys. Rev. Lett. **87**, 067202 (2001).
[8] S. A. Kivelson, D.-H. Lee, E. Fradkin, and V. Oganesyan, Phys. Rev. B **66**, 144516 (2002).
[9] A. B. Vorontsov, M. G. Vavilov, and A. V. Chubukov, Phys. Rev. B **79**, 060508(R) (2009).
[10] Z. Nussinov, I. Vekhter, and A. V. Balatsky, Phys. Rev. B **79**, 165122 (2009).
[11] A. J. Millis, Phys. Rev. B **81**, 035117 (2010).
[12] R. M. Fernandes and J. Schmalian, Phys. Rev. B **82**, 014521 (2010).
[13] E. G. Moon and S. Sachdev, Phys. Rev. B **82**, 104516 (2010).
[14] J.-H. She, J. Zaanen, A. R. Bishop, and A. V. Balatsky, Phys. Rev. B **82**, 165128 (2010).
[15] D. Chowdhury, E. Berg, and S. Sachdev, Phys. Rev. B **84**, 205113 (2011).
[16] B. Lake, G. Aeppli, K. N. Clausen, D. F. McMorrow, K. Lefmann, N. E. Hussey, N. Mangkorntong, M. Nohara, H. Takagi, T. E. Mason, and A. Schroder, Science **291**, 1759 (2001).
[17] B. Lake, H. M. Ronnow, N. B. Christensen, G. Aeppli, K. Lefmann, D. F. McMorrow, P. Vorderwisch, P. Smeibidl, N. Mangkarntong, T. Sasagawa, M. Nohara, H. Takagi, and T. E. Mason, Nature (London) **415**, 299 (2002).
[18] J. E. Hoffman, E. W. Hudson, K. M. Lang, V. Madhavan, H. Eisaki, S. Uchida, and J. C. Davis, Science **295**, 466 (2002).
[19] C.-L. Song, Y.-L. Wang, P. Cheng, Y.-P. Jiang, W. Li, T. Zhang, Z. Li, K. He, L.-L. Wang, J.-F. Jia, H.-H. Hung, C.-J. Wu, X.-C. Ma, X. Chen, and Q.-K. Xue, Science **332**, 1410 (2011).
[20] J. Hertz, Phys. Rev. B **14**, 1165 (1976).
[21] A. J. Millis, Phys. Rev. B **48**, 7183 (1993).
[22] T. Moriya, *Spin Fluctuations in Itinerant Electron Magnetism* (Springer-Verlag, Berlin, New York, 1995).
[23] D. Belitz, T. R. Kirkpatrick, and T. Vojta, Phys. Rev. B **55**, 9452 (1997).
[24] A. V. Chubukov, C. Pépin, and J. Rech, Phys. Rev. Lett. **92**, 147003 (2004); J. Rech, C. Pépin, and A. V. Chubukov, Phys. Rev. B **74**, 195126 (2006).
[25] A. Abanov and A. V. Chubukov, Phys. Rev. Lett. **93**, 255702 (2004).
[26] P. Strack, S. Takei, and W. Metzner, Phys. Rev. B **81**, 125103 (2010); S. C. Thier and W. Metzner, Phys. Rev. B **84**, 155133 (2011).
[27] G.-Z. Liu, J.-R. Wang, and J. Wang, Phys. Rev. B **85**, 174525 (2012).
[28] Y. Ando, K. Segawa, S. Komiya, and A. N. Lavrov, Phys. Rev. Lett. **88**, 137005 (2002).
[29] V. Hinkov, D. Haug, B. Fauque, P. Bourges, Y. Sidis, A. Ivanov, C. Bernhard, C. T. Lin, and B. Keimer, Science **319**, 597 (2008).
[30] R. Daou, J. Chang, D. LeBoeuf, O. Cyr-Choiniere, F. Laliberte, N. Doiron-Leyraud, B. J. Ramshaw, R. Liang, D. A. Bonn, W. N. Hardy, and L. Taillefer, Nature (London) **463**, 519 (2010).
[31] M. J. Lawler, K. Fujita, Jhinhwan Lee, A. R. Schmidt, Y. Kohsaka, Ch. K. Kim, H. Eisaki, S. Uchida, J. C. Davis, J. P. Sethna, and E.-A. Kim, Nature **466**, 347 (2010).
[32] S. A. Kivelson, E. Fradkin, and V. J. Emery, Nature (London), **393**, 550 (1998).
[33] C. J. Halboth and W. Metzner, Phys. Rev. Lett. **85**, 5162 (2000); W. Metzner, D. Rohe, and S. Andergassen, Phys. Rev. Lett. **91**, 066402 (2003). L. Dell'Anna and W. Metzner, Phys. Rev. B **73**, 045127 (2006).
[34] V. Oganesyan, S. A. Kivelson, and E. Fradkin, Phys. Rev. B **64**, 195109 (2001).
[35] M. Vojta, Y. Zhang, and S. Sachdev, Phys. Rev. B **62**, 6721 (2000); Phys. Rev. Lett. **85**, 4940 (2000).
[36] E.-A. Kim, M. J. Lawler, P. Oreto, S. Sachdev, E. Fradkin, and S. A. Kivelson, Phys. Rev. B **77**, 184514 (2008).
[37] Y. Huh and S. Sachdev, Phys. Rev. B **78**, 064512 (2008).
[38] C. Xu, Y. Qi, and S. Sachdev, Phys. Rev. B **78**, 134507 (2008).
[39] L. Fritz and S. Sachdev, Phys. Rev. B **80**, 144503 (2009).
[40] E.-A. Kim and M. J. Lawler, Phys. Rev. B **81**, 132501

(2010).

[41] J. Wang, G.-Z. Liu, and H. Kleinert, Phys. Rev. B **83**, 214503 (2011).

[42] R. Shankar, Rev. Mod. Phys. **66**, 129 (1994).

[43] J. Orenstein and A. J. Millis, Science **288**, 468 (2000).

[44] M. Chiao, R. W. Hill, Ch. Lupien, L. Taillefer, P. Lambert, R. Gagnon, and P. Fournier, Phys. Rev. B **62**, 3554 (2000).

[45] P. A. Lee, Phys. Rev. Lett. **71**, 1887 (1993).

[46] A. Durst and P. A. Lee, Phys. Rev. B **62**, 1270 (2000).

[47] P. A. Lee and X.-G. Wen, Phys. Rev. Lett. **78**, 4111 (1997); A. Paramekanti and M. Randeria, Phys. Rev. B **66**, 214517 (2002).

[48] B. I. Halperin, T. C. Lubensky, and S.-K. Ma, Phys. Rev. Lett. **32**, 292 (1974).

[49] E. Domany, D. Mukamel, and M. E. Fisher, Phys. Rev. B **15**, 5432 (1977); J. Rudnick, Phys. Rev. B **18**, 1406 (1978); J.-H. Chen and T. C. Lubensky, Phys. Rev. B **17**, 4274 (1978).

[50] J. Cardy, *Scaling and Renormalization in Statistical Physics* (Combridge University Press, Combridge, UK, 1996).